Journal of Environmental Management 289 (2021) 112563

Contents lists available at ScienceDirect

Journal of Environmental Management

journal homepage: http://www.elsevier.com/locate/jenvman

Research article

Ecological risk potentials of petroleum hydrocarbons and heavy metals shape the bacterial communities of marine hydrosphere at Atlantic Ocean, Atlas Cove, Nigeria

Ganiyu O. Oyetibo [*], Oluwatobi O. Ige [1], Peace K. Obinani [1], Olukayode O. Amund [2]

Department of Microbiology, Faculty of Science, University of Lagos, Akoka, Yaba, Lagos State, 101017, Nigeria

ARTICLE INFO

Keywords:
Atlantic ocean
Petroleum
Pollution
Ecological risk
Bacterial community

ABSTRACT

Trans-Atlantic voyage of petroleum often leads to marine pollution with petroleum hydrocarbons (PHs) and heavy metals (HMs) that defines structures of autochthonous bacteria in the hydrosphere. Bacterial taxa of marine sediments exposed to petroleum transport activities were profiled using 16S rDNA metagenomics and correlated with the geochemistry to establish their impact on the microbiome. The physico-chemistry of the marine systems revealed varied degrees of contamination with PHs and HMs exceeding recommended threshold for aquatic life. Ecological risk assessment based on organic carbon of the sediment established phenanthrene, anthracene, and pyrene posed high risks (index risk quotient >32) to marine life. The most dominant phylum of the 44 bacterial phyla in the marine-sphere was Proteobacteria with relative abundance of 45–77% in the sampling locations. Relative dominance of Proteobacteria in the sediments spanned Gammaproteobacteria (17–25%), Deltaproteobacteria (12–20%), and Alphaproteobacteria (7–14%). Whereas, more operational taxonomic units (OTUs) belonging to Epsilonproteobacteria (19 ± 2.4%) were found in estuarine sediment unlike < 0.5% relative abundances obtained from oceanic sediments. *Sulfurimonas* apparently dominated the bacterial genera with up to 2.16 ± 0.19% abundance in oceanic sediments. Canonical correspondence analysis revealed that PHs shaped the structure of bacterial OTUs in oceanic sediments where petroleum loading/offloading occurs unlike in some kilometres a yonder where HMs correlated with the bacteria structure. The dominant bacteria might possibly pivotal to ecophysiologies of hydrocarbon contaminated marine environment, and would be pertinent to biotechnological applications for possible bioremediation campaign.

1. Introduction

Petroleum comprising hydrocarbons and heavy metals (HMs), like other hazardous chemical products, is shipped in large quantities over the oceanic waters. Major sources of pollution of global oceans with petroleum hydrocarbons (PHs) and associated HMs include catastrophic spills upon tanker accident and leakages from pipeline during high sea loading and off-loading petroleum products. Approximately 1.3 million tons of PHs and HMs enter the marine environment each year (Ventikos and Sotiropoulos, 2014), where they sink, settle down and adsorb to solid matrix in the marine sediments (Duran and Cravo-Laureau, 2016; Reddy et al., 2004). Presence of PHs and HMs in marine hydrosphere causes direct and indirect serious impact on human and ocean health at sites near or remote from the sources of discharge. Consequently, cellular physiologic conditions in oceans are altered upon bioaccumulation of PHs and HMs from the water column leading to disturbances in metabolic reactions and hormone imbalance in life forms (Desforges et al., 2016). Acute necrosis mortality, mutagenicity, hypothermia, smothering, drowning and tissue loss are some of the short-term impacts of multiple acute and chronic exposures of marine life to PHs and HMs (Desforges et al., 2016).

Petroleum contamination significantly shapes and forms the diversity of aboriginal bacterial communities in marine environment (Head et al., 2006), causing significant loss of diversity and a shift in the composition towards dominance of species that metabolise and/or sequester the petroleum stressors (Catania et al., 2018). More

* Corresponding author.
E-mail address: goyetibo@unilag.edu.ng (G.O. Oyetibo).
[1] Graduate students at the period of study and have completed their degree. The findings constitute parts of their dissertations.
[2] Current address: Office of the Vice Chancellor, Elizade University, Ilara-Mokin, Ondo State, Nigeria.

https://doi.org/10.1016/j.jenvman.2021.112563
Received 25 January 2021; Received in revised form 26 March 2021; Accepted 3 April 2021
Available online 11 April 2021

importantly, bacterial shift due to PHs and HMs input causes selective pressures that result in a concomitant enrichment and evolution of hydrocarbonoclastic genera that tolerate or transform HMs to innocuous forms (Acosta-Gonzalez and Marques, 2016; Oyetibo et al., 2017; Rosano-Hernandez et al., 2012). Some of the hydrocarbonoclastic bacterial genera, including *Oleispira, Marinobacter, Thalassolituus, Alcanivorax* and *Cycloclasticus,* are present at low or undetectable levels before pollution, but found to dominate oil-polluted marine systems after PHs pollution (Brooijmans et al., 2009). On the contrary, *Acinetobacter, Pseudomonas, Rhodococcus, Bacillus* found in abundance in the unpolluted marine system, increase their dominance after PHs pollution due to up-regulation of hydrocarbon degradation and/or HMs sequestration genes (Oyetibo et al., 2013, 2017; Varjani, 2017). In maintaining the ocean health, hydrocarbonoclastic bacterial taxa drive natural attenuation processes upon utilising PHs for carbon and energy supply to cellular physiology (Catania et al., 2015), while the HMs-resistant species sequester HMs to innocuous forms (Oyetibo et al., 2010, 2019). Many members of hydrocarbonoclastic bacteria do overcome hydrophobicity and poor bio-accessibility nature of PHs through activities of surface-active compounds they synthesize (Barin et al., 2014; Obayori et al., 2009), but some others directly uptake PHs along with HMs (Oyetibo et al., 2013).

The bacterial community structure of marine sediment as it relates with the inherent geochemical risks of the environment can serve as an indicator of marine health. Subtle changes in the environment resulting from anthropogenic perturbations from petroleum contaminations do silhouette the bacterial diversity. It has been reported that elevated levels in species richness and diversities in impacted environment contribute to exceptional functionalities within the microbiome and possible recovery during eco-toxicological stress that leads to promoting health of the ecosystem (She et al., 2017). Knowledge about influence of eco-toxicants on bacterial community structure of oceanic sediments where PHs and HMs co-exist is sought in this study. Therefore, the specific objectives of the present study include: (1) to profile and compare the composition and structure of the bacterial communities in the marine sediments exposed to petroleum contamination during ship loading/offloading, and (2) to explore the potential correlations between the prevailing geochemical factors and the bacterial communities as determined by the forms and diversities of the marine bacteria. The outcome of this work would therefore suggest prospective autochthonous bacterial profiles that are key players in the contaminated marine. As such, linking bacterial community composition and structure with geochemical variables would be cogent to amelioration strategies of marine systems that are polluted with petroleum.

2. Materials and method

2.1. Site description and sampling

The Atlas Cove jetty, owned and managed by the Pipelines and Products Marketing Company (PPMC) on behalf of Nigerian National Petroleum Corporation (NNPC), is on the Commodore Channel at 'Takwa Bay' of the Atlantic Ocean in Lagos, Nigeria. The jetty housed a major petroleum facility, which is Nigeria's major delivery and redistribution point for refined petroleum products. The jetty is a storage farm/facility that channels refined products through system 2B pipelines, which runs through conurbation in Lagos, and the entire Southwestern region of Nigeria. The jetty frequently experiences petroleum spills into the Atlantic Ocean occasioned by accidental discharges from pipeline leaks during petroleum loading and/or offloading from vessels. Sampling locations were petroleum loading facility at Atlas Cove on the Atlantic Ocean (ATL1: 6° 23′54" N 3° 23′46" E); and a location on shore (approx. 2 km) away from the facility (ATL2: 6° 24′31" N 3° 23′38" E). Also, an off shore (1 km off the Atlantic Ocean), to the west of the facility, lays a portion of extensive brackish water and creeks along the coastline of the Gulf of Guinea (ATL3: 6° 24′49" N 3° 23′14" E). Water and sediment samples (10 composite at each location) were collected in sterile glassware aseptically, using a van Veen grab that had been surfaced sterilised with absolute ethanol and flamed, and samples were transported to the laboratory inside ice-packed cooler within 24 h for analysis.

2.2. Analysis of environmental factors

Physico-geochemical parameters of the samples were determined by standard methods earlier reported (Oyetibo et al., 2019). While pH and dissolved oxygen (DO) were determined *in situ*, physico-chemical assays determined *ex situ* include electrical conductivity, turbidity, chlorides, chemical oxygen demand (COD), and biochemical oxygen demand (BOD), total solids (TS), total dissolved solids (TDS), total suspended solids (TSS), nitrate, sulphate, phosphate, total hardness, oil and grease, alkalinity, acidity, total organic carbon (TOC), total organic matter (TOM), and cation-exchange capacity (CEC) as applicable. Seven HMs including lead (Pb), cadmium (Cd), zinc (Zn), copper (Cu), iron (Fe), nickel (Ni), and chromium (Cr) were quantified via atomic absorption spectrophotometry (AAS-Perkin-Elmer Analyst 200; Pelkin-Elmer, Canada) after sample (0.1 g) digestion with $HNO_3/HClO_4$ (4:1, v/v) in a microwave oven (Oyetibo et al., 2010). Standards of HMs concentrations ranging 0–100 mg/l were prepared from multi-element calibration standard-2A solution (Agilent Technologies). AAS normalisation, validation, operational conditions and the limit of detection were as earlier reported (Ogwugwa et al., 2020). The wavelengths used for Cd, Pb, Ni, Cr, Fe, Zn and Cu measurements were 228.8, 283.3, 231.1, 357.9, 248.3, 213.9 and 324.8 nm analytical lines, respectively. Extractions of PHs and PAHs from samples (water and sediments), and consequent analysis of the reconstituted organic phase of the extract (1.0 μl) upon injection into HP 5890 Series II gas chromatograph (Hewlett Packard, Wilmington, DE, USA) fitted with flame ionization detector (FID) and an Agilent J & W Scientific DB-1 fused silica 30 m long column (internal diameter, 0.32 mm; film thickness, 1.0 μm) (Agilent Technologies, Santa Clara CA, USA) were as earlier reported (Oyetibo et al., 2017; Sogbamu et al., 2019).

2.3. Community DNA extraction, purification and quantification

Approximately 0.5 g dry weight of sediments was subjected to total community DNA (tcDNA) extraction, using FastDNA® Spin Kit for Soil (MP Biomedicals, Solon, OH, USA) according to the manufacturer instructions in combination with the FastPrep® Cell Disruptor FP 120 (Qbiogene, Heidelberg, Germany). To prevent interference of humic substances in tcDNA with polymerase chain reactions (PCR), 40 mg of skim milk per gram of sediment sample was added to the lysing matrix as earlier reported (Oyetibo et al., 2019). The Cell Disruptor was operated at 6.0 speed for 40 s in order to achieve a harsh cell wall disruption. The yield, quality and purity of tcDNA was checked with Nano-Drop spectrophotometry along with 0.8% (w/v) agarose gel electrophoresis and visualized in UV light upon staining with ethidium bromide.

2.4. High throughput sequencing and analysis of sequence reads

Amplification of the V1 to V3 regions of bacterial 16S rRNA gene, subsequent preparation of library and sequencing with Illumina MiSeq system (Illumina, San Diego, CA, USA) were performed at ChunLab Inc., Seoul, Korea. Processing of sequencing data, detection of chimeric sequences, and taxonomical assignment of each sequence reads were according to BIOiPLUG in-house pipeline where UCHIME was used to detect and remove chimera against chimera-free reference database. Taxonomic assignment was carried out by comparing the sequence reads against the EzBioCloud 16S database (https://www.ezbiocloud.net/), using a combination of the initial BLAST-based searches and additional pairwise 97% similarity comparisons as the cutoff (Yoon et al., 2017). The taxonomic assignment of each read was based on the criterion

reported by Nguyen et al. (2016). A read was assigned to an unclassified group if the distance was greater than the cut-off value (0.97). Sequence abundance data per cluster was transformed to relative abundance (as a percentage of the total number of sequence per sample). Further bioinformatics analysis of sequencing data was performed using CLcommunity™ software package (ChunLab Inc., Seoul, Korea) following manufacturer's instructions. The Illumina sequencing reads obtained in this study (BioProject number **PRJNA522867**) have been deposited in the NCBI's sequence read archive (SRA) database under SRA accession number **PRJNA522867.**

2.5. Statistical analysis

All geochemical measurements of environmental samples were performed in three replicates where mean of values and standard error of mean (SEM) were performed using the Prism 5 software program (GraphPad Software, San Diego, CA, USA). The estimated coverage of the constructed 16S rRNA gene libraries was calculated as: $C = 1 - (\frac{n}{N}) \times 100$ according to Kemp and Aller (2004), where n is the number of Singletons after assembly and N is the total number of sequences in the initial dataset. Richness and diversity statistics of the bacterial community including abundance-based coverage estimator (S_{ACE}), the bias-corrected Chao1 (Scha o1) and the Shannon-Weaver diversity index were estimated using pre-calculated program of CLcommunity™ software package. The un-weighted pair group method with the arithmetic mean (UPGMA) was also performed on the weighted-normalized UniFrac calculation. The principal coordinate analysis (PCoA), Heat maps of core bacterial taxa and canonical correspondence analysis (CCA) were performed using the CLcommunity™ software package to visualise how bacterial community relates with the prevailing environmental factors. All statistical tests were considered significant at $p < 0.05$.

3. Results

3.1. Environmental factors and ecological risk assessments of the sampling locations

The values of physico-chemistry, HMs and PHs as evident with the PAHs measures vividly revealed gross contaminations of the sampling locations (Table 1). While environmental guidelines of permissible limits of many of the measured parameters were not available, the water quality of the three locations as determined by turbidity (17.9–35.1 NTU), chloride (4630–7340 mg/l) and total suspended solids (3030–4810 mg/l) (see Table A1 in the supplementary document) were far above recommendations for the protection of aquatic life. Moreover, contents of HMs in the waters appeared not hazardous to aquatic life unlike the concentrations of naphthalene (1.66–6.73 mg/l), acenalphthene (0.63–3.5 mg/l), and anthracene (3.27–69.7 mg/l) that were above recommended guidelines for the protection of aquatic life in all the hydrosphere (Table 1). However, concentrations of Cd (3.0–4.01 mg/kg), and Cu (23.0–26.2) in the sediments were apparently beyond the values recommended by guidelines for aquatic life. Those PAHs that exceeded recommended concentrations in sediments were fluorene (0.09–1.06 mg/kg) in all the locations, phenanthrene (0.2 mg/kg) in ATL1, and pyrene (>1.0 mg/kg) in ATL1 and ATL3 (Table 1). The ecological risk assessments of PAHs (as indicators of PHs) and the associated HMs were based on the characterisation of the potential risks of the toxicants as determined by the index risk quotient (RQ). This was calculated by:

$$RQ = \frac{C_e}{(\frac{C_{sed}}{C_{wat}}) \times F_{oc}}. \quad (1)$$

where C_e (mg/l) is the measured environmental concentration, C_{sed} is the toxicant concentration in the sediment, C_{wat} is toxicant

Table 1
Geochemical characteristics of water and sediments of the impacted Atlas Cove (ATL1), the adjacent ocean (ATL2) and estuary (ATL3).

Parameters	Water (mg l^{-1})			Sediment (mg kg^{-1})			Quality guidelines	RQ		
	ATL1	ATL2	ATL3	ATL1	ATL2	ATL3		ATL1	ATL2	ATL3
Heavy Metals										
Lead (Pb)	0.34 (0.33)	0.13 (0.06)	3.0 (2.95)	19.6 (3.52)	15.9 (3.34)	5.75 (2.38)	0.01[a]	0.21	0.08	1.8
Cadmium (Cd)	0.001	0.004 (0.003)	2.87 (2.86)	**3.0 (0.29)**	**4.01 (0.29)**	**3.44 (1.66)**	0.7[s**]	0.0006	0.002	1.74
Zinc (Zn)	8.52 (8.24)	17.5 (17.3)	23.0 (22.5)	101.0 (76.7)	152.0 (74.2)	106.0 (72.3)	3.0[a]	5.2	11	14
Copper (Cu)	3.75 (3.63)	4.15 (3.93)	23.1 (23.0)	**23.0 (4.07)**	**26.2 (5.12)**	**23.2 (8.92)**	18.7[s**]	2.3	2.5	14
Iron (Fe)	0.87 (0.18)	1.21 (0.46)	1.45 (0.6)	409 (297)	202 (1.7)	736 (583)	0.3[a]	0.53	0.73	0.88
Nickel (Ni)	4.02 (3.99)	4.1 (3.95)	6.7 (6.65)	25.2 (10.3)	19.9 (1.79)	25.1 (4.65)	0.02[a]	2.4	2.5	4.1
Chromium (Cr)	3.3 (2.81)	2.25 (2.12)	3.33 (2.27)	15.4 (4.04)	14.6 (2.94)	10.3 (1.93)	52.3[s**]	2.0	1.4	2.0
RQ_{mic} of heavy metals								**12.64**	**18.21**	**38.52**
PAHs										
Naphthalene	**6.73 (0.15)**	**5.96 (0.17)**	**1.66 (0.33)**	0.58 (0.21)	0.7 (0.31)	0.67 (0.28)	0.0014[b]	4.1	3.6	1.0
Acenaphthylene	BDL	BDL	BDL	0.34 (0.17)	0.63 (0.63)	0.87 (0.44)	0.19[b]	ND	ND	ND
Acenalphthene	**3.5 (0.25)**	**0.82 (0.13)**	**0.63 (0.3)**	0.02 (0.02)	0.08 (0.07)	0.14 (0.07)	0.089[b]	2.1	0.49	0.38
Fluorene	0.08 (0.08)	0.02 (0.02)	1.0 (0.01)	**0.3 (0.26)**	**0.09 (0.08)**	**1.06 (0.6)**	0.021[s**]	0.05	0.01	0.06
Phenanthrene	73.2 (4.08)	17.9 (2.76)	1.61 (0.69)	**0.2 (0.16)**	0.07 (0.02)	0.04 (0.02)	0.087[s**]	44	11	1.0
Anthracene	**69.7 (8.2)**	**18.7 (0.72)**	**3.27 (1.05)**	0.16 (0.14)	0.15 (0.15)	1.27 (1.0)	0.25[b]	42	11	2.0
Pyrene	54.6 (5.16)	18.4 (2.96)	0.89 (0.12)	**1.63 (1.5)**	0.05 (0.04)	**2.53 (1.58)**	0.15[s**]	33	11	0.54
Benz(a)anthracene	0.34 (0.34)	0.02 (0.02)	**22.9 (1.45)**	1.16 (0.72)	0.26 (0.26)	0.51 (0.26)	0.69[b]	0.21	0.01	14
Dibenz(ah)anthracene	0.33 (0.33)	0.34 (0.34)	0.03 (0.03)	BDL	BDL	BDL	0.006[s**]	–	–	–
Total PAHs	380 (126)	116 (37.4)	58 (19.4)	24 (8.07)	3.77 (1.23)	15.6 (4.42)		230	70	35
RQ_{mic} of PAHs								**125.46**	**37.11**	**18.98**
RQ_{mic} of all toxicants								**138.1**	**55.32**	**57.5**

s**Marine sediment quality guidelines for the protection of aquatic life (Canadian Council of Ministers of the Environment, CCME).
Values represent mean of replicate analyses with the standard error mean appeared in the parentheses. Values in bold indicate above recommended limit of UNEP. BDL = below detection level; - = not applicable.
[a] Recommended limits set by WHO.
[b] Marine water quality guidelines for the protection of aquatic life (Canadian Council of Ministers of the Environment, CCME).

concentration in water, and F_{oc} is the organic carbon in the sediment. A RQ ≥ 1 shows the risk posed by toxicants is high but the risk is low if RQ < 1. The calculated RQ values of HMs and the PAHs as listed in Table 1 indicated that zinc, copper, nickel and chromium posed high risk to life in all the sediments unlike other HMs with low eco-risk. Furthermore, naphthalene, acenalphthene, phenanthrene, and anthracene appeared to pose high risks to aquatic life in the marine sediments. Interestingly, pyrene seemed to pose extremely high risk to life in the sediments of ATL1 and ATL2 unlike low ecological risk observed in ATL3 sediments. Moreover, the mixture toxicity RQ_{mix} of all the toxicants in the marine environment that shape the microbiome was calculated using the model of concentration addition whereby their risk quotients were summed up as:

$$\sum_{i-1}^{n} RQ_i = \sum_{i-1}^{n} \frac{C_e}{\left(\frac{C_{sed}}{C_{wat}}\right) \times F_{oc}} \quad (2)$$

Thus, the toxicants or groups of toxicants of greatest concerns to shaping the bacterial community of the marine system were identified upon comparing RQ_i of single compounds to the total risk of the RQ_{mix}. As depicted in Table 1, the marine environments were postulated to be exposed to extreme risk doses of coexisting heavy metals and PAHs (ATL1, 138.1; ATL2, 55.32; and ATL3, 57.5). Specifically, the estuarine system (ATL3) was speculated to be mostly impacted with HMs mixture ($RQ_{mic} = 38.52$), while potential toxicological impact of PHs was most extreme at the oceanic system where the petroleum loading facility was located (ATL1: $RQ_{mic} = 125.46$).

3.2. Bacterial community profiling of sediments

3.2.1. Bacterial taxonomic composition

Quality treatment of sequencing data yielded highest valid reads of bacteria in ATL3 (89,100 ± 1080) and the least with 61,200 (±35,400) in ATL1, while the highest number of OTUs was found in the valid sequence reads of ATL2 (13,900 ± 837) as shown in Table 2. Composition of phyla varied in the samples as presented in Fig. 1. Further, relative abundances of the phyla in relation to the genera across the sediments were shown as double pie chart in the supplementary document (Fig. A1). A total of 44 phyla were observed in all the samples where sum sequences of 11 of the phyla were ≥5.0%. Of these 11 phyla, recently identified Latescibacteria_WS3 was found to comprise 1.7 ± 0.4%, 1.4 ± 0.04% and 0.13 ± 0.03% of the total valid reads in ATL1, ATL2 and ATL3, respectively. The dominant phylum in all the samples was Proteobacteria with relative abundance of 77 ± 1.4% in the estuarine ATL3. Whereas, 45 ± 4.8% and 47 ± 1.1% of bacteria in oceanic ATL1 and ATL2 sediments, respectively, were Proteobacteria. Other phyla found across all the samples with sum sequence ≥10% include Chloroflexi, Plantomycetes, Acidobacteria, Actinobacteria and Bacteriodetes (Fig. 1). Unidentified phyla found in all the sample with sum sequences less than 5.0% include Parcubacteria_OD1, Aminicenantes_OP8, GN04, Caldithrix_p, Omnitrophica_OP3, Hydrogenedentes_NKB19, BRC1, TM6, Cloacamonas_p, Microgenomates_OP11, Acetothermia_OP1, Saccharibacteria_TM7, EU652510_p, Marinimicrobia_SAR406, JMYB36, WWE3, GU363019, and Bacteria_uc.

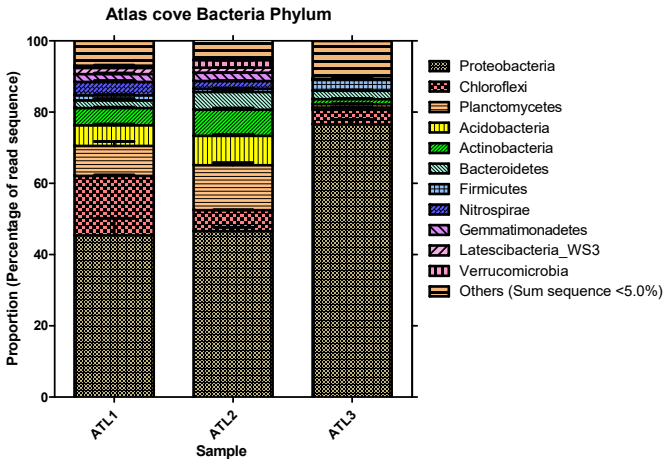

Fig. 1. Phylum-level taxonomic composition of oceanic (ATL1 and ATL2) and estuarine (ATL3) sediments. Phyla whose sum sequences are less than 5.0% of the total sequence reads were regarded as 'Others'. Error bars are standard error of the mean for replicate samples.

Table 2
Alpha diversity estimates of bacterial richness and diversity in the sediments.

		ATL1	ATL2	ATL3
Valid reads		61,200 (35,400)	78,000 (1590)	89,100 (1080)
OTUs		11,400 (4370)	13,900 (837)	6440 (697)
Ace	Actual	11,500 (4380)	14,000 (840)	6500 (705)
	HCI	11,500 (4380)	14,000 (840)	6520 (707)
	LCI	11,500 (4380)	14,000 (840)	6480 (704)
Chao1	Actual	11,400 (4370)	13,900 (837)	6450 (698)
	HCI	11,400 (4370)	13,900 (836)	6460 (698)
	LCI	11,400 (4370)	13,900 (837)	6440 (698)
JackKnife	Actual	11,700 (4420)	14,200 (840)	6630 (721)
	HCI	11,700 (4420)	14,200 (840)	6630 (721)
	LCI	11,700 (4420)	14,200 (840)	6630 (721)
NPShannon		8.9 (0.06)	9.0 (0.08)	6.4 (0.2)
Shannon	Actual	8.5 (0.2)	8.6 (0.06)	6.3 (0.2)
	HCI	8.5 (0.2)	8.6 (0.06)	6.3 (0.2)
	LCI	8.5 (0.2)	8.6 (0.06)	6.2 (0.2)
Simpson	Actual	0.001 (0.00008)	0.001 (0.00008)	0.014 (0.003)
	HCI	0.002 (0.0001)	0.001 (0.00004)	0.014 (0.003)
	LCI	0.001 (0.00004)	0.001 (0.00004)	0.013 (0.0029)
Goods Lib. Coverage		99.3 (0.3)	99.6 (0.006)	99.8 (0.024)

OTUs = Operational taxonomic units, determined by clustering method of CD-HIT at 97%; HCI = High Confidence Interval (95%); LCI = Low Confidence Interval (95%); ATL1 = Sediments from the petroleum loading/offloading platform at Atlas Cove, Atlantic Ocean; ATL2 = Oceanic sediments 2 km away from ATL1; ATL3 = Estuarine sediment; Richness and diversity were determined with CD-HIT clustering method. Values represent mean of replicate analyses with the standard error mean appeared in the parentheses.

As shown in Fig. 2, eight classes of bacterial taxa among others in the sediments were dominant based on heat map analysis using OrthoAni values of the Fast UniFrac metric. Four most dominant classes in the bacterial taxa belong to Proteobacteria, of which Gammaproteobacteria (ATL1: 17 ± 4%; ATL2: 25%; and ATL3: 22 ± 3.4%), Deltaproteobacteria (ATL1: 20 ± 0.3%; ATL2: 13 ± 1.2; and ATL3: 12 ± 1.9%), and Alphaproteobacteria (ATL1: 7.0 ± 0.23; ATL2: 7.7 ± 0.24; and ATL3: 14 ± 0.9%) appeared evenly distributed in the samples. Whereas, Epsilonproteobacteria composition tilted towards ATL3 (19 ± 2.4%) unlike < 0.5% relative abundances of sequence reads observed in ATL1 and ATL2 sediments (Fig. A2). The phylogenies of dominant bacterial taxa showing the evolutionary relatedness of common OTUs both ATL1 and ATL2, as well as those OTUs exclusively dominant in each of the oceanic locations are shown in Fig. 3. The 20 most dominant genera revealed unclassified *DQ811856_g* (4.1%), *Woeseia* (6.09%) and *Sulfurimonas* (17.6%) as most abundant genera in ATL1, ATL2 and ATL3, respectively (See supplementary material, Table A2). Interestingly, more than half of the 20 most dominant genera in all the samples were unidentified. Despite close relationships of ATL1 and ATL2 away from ATL3 as delineated by the OrthoAni scale (Fig. 2), Taxon XOR analysis by CD-HIT program revealed that 146 genera were present in ATL1 but absent in ATL2, while 726 genera present in ATL1 were missing in ATL3. Likewise, 210 genera present in ATL2 were apparently not found in ATL1,

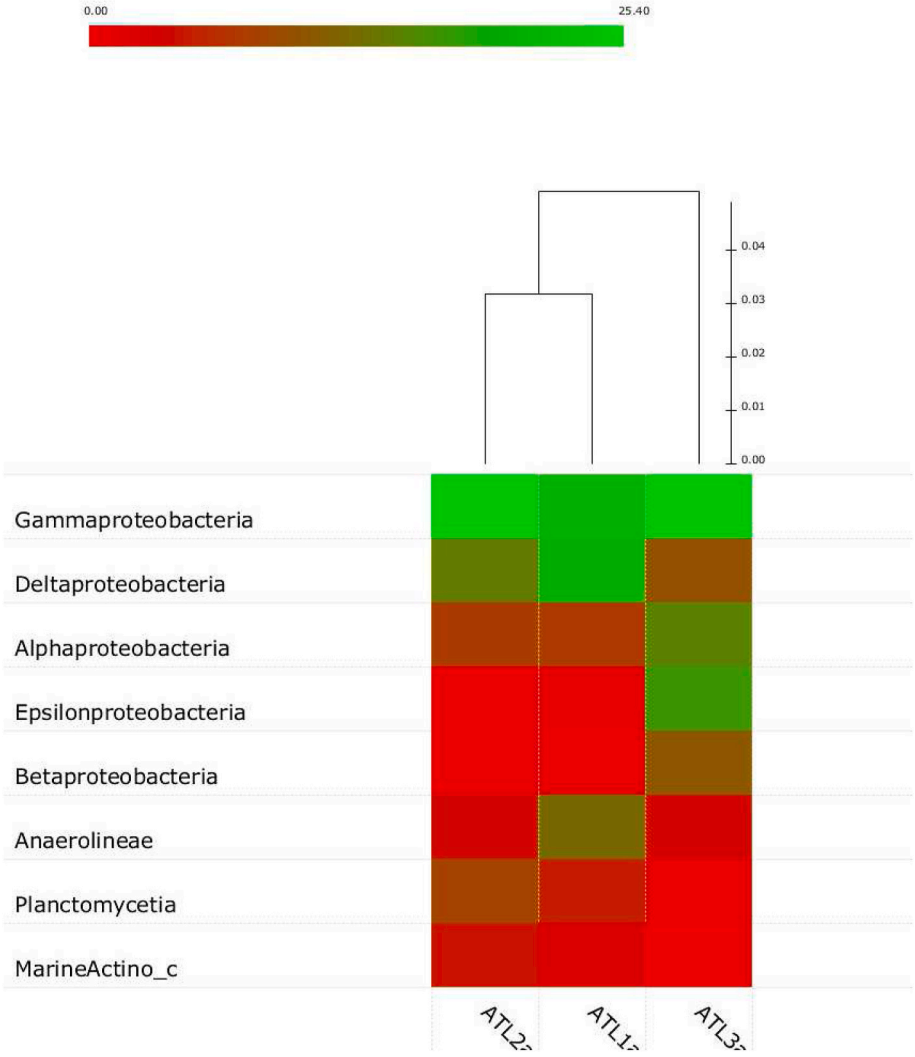

Fig. 2. Heat map (gradient) representing abundance of eight bacterial families that is above the cut off. Each taxon and its proportion are represented by a square and relativity of samples based on operational taxonomic units (OTUs) delineated by the OrthoAni scale is shown as dendogram. The full size of square equals 25.4%.

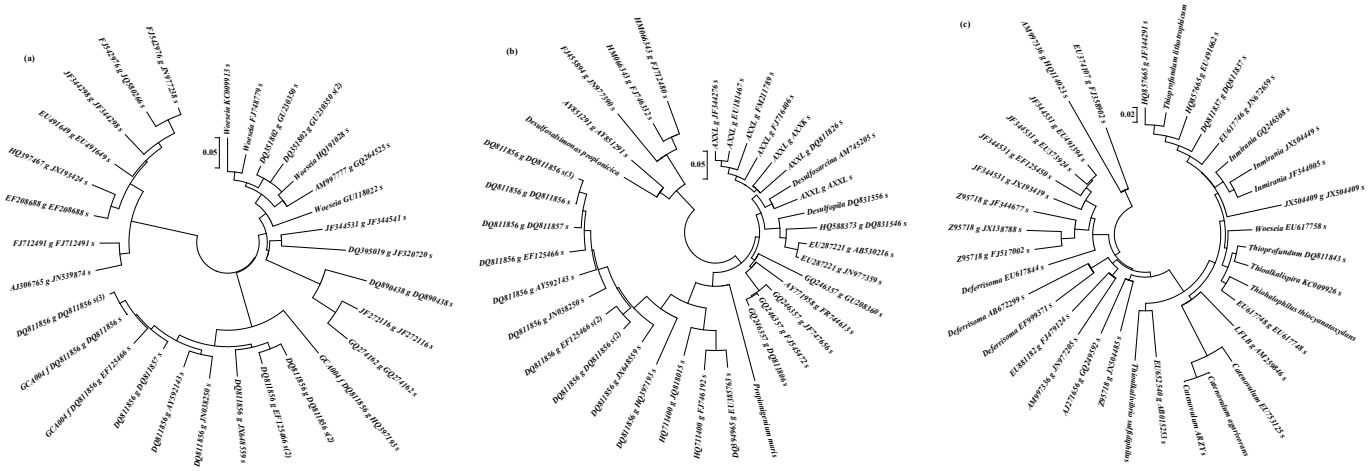

Fig. 3. Evolutionary relationships of dominant bacteria taxa common to both ATL1 and ATL2 (a), exclusively dominant in ATL1 (b), and exclusively dominant in ATL2 (c) locations of Atlantic Ocean. The evolutionary history was inferred using the Neighbor-Joining method. The optimal tree with the sum of branch length equals 1.82, 2.23 and 2.09 is shown for Panel a, b and c, respectively. The unrooted trees were drawn to scale, with branch lengths in the same units as those of the evolutionary distances used to infer the phylogenetic tree using MEGA6. The evolutionary distances were computed using the Maximum Composite Likelihood method and are in the units of the number of base substitutions per site.

just as 412 genera that existed in ATL3 could not be found in ATL1. However, 978 genera that were vividly present in ATL2 were missing in ATL3 and vice versa, 422 genera found in ATL3 were absent in ATL2. It is noteworthy that the genera found in the samples were predominantly not yet identified.

3.2.2. Bacterial richness and alpha diversity statistics of the bacterial community

Operational taxonomy units (OTUs) in the samples, detected via taxonomy-dependent clustering (TDC) followed by a taxonomy-based clustering (TBC), were depicted with rarefaction curves that compared OTU richness among the samples (Fig. A3). None of the curves reached an asymptote nor did they overlap as 95% confidence intervals of the curves were applied. The rarefaction curves revealed that ATL2 reached the highest number of OTUs per sequence reads followed by ATL1, while ATL3 attained the least number of OTUs per sequence reads. Estimations of bacterial richness and diversity are summarised in Table 2. Goods libraries coverage estimator revealed that more than 99% of the sequences in all the samples represented the bacteria present in the sediments. The bacterial richness and diversity appeared closely related with marginal differences in the two locations of the Atlantic Ocean (ATL1 and ATL2) unlike what was estimated in the estuarine ecosystem (ATL3). The sediments from the Atlantic Ocean (ATL1 and ATL2) had richer bacterial OTUs than ATL3, where ATL2 contained highest OTUs as estimated with Ace, Chao1 and JackKnife (Table 2). Similarly, Shannon-Weaver diversity indexes represented by NPShannon and Shannon values showed that ATL2 contained the most diverse OTUs, closely followed by ATL1 while ATL3 was the least diverse. OTUs estimated for ATL1 and ATL2 sediments were more complex and diverse than ATL3 by more than 10^3.

3.3. Beta diversities and geochemical factors that shape bacterial communities of contaminated marine sediments

The unweighted pair group method and arithmetic mean (UPGMA) dendogram based on Fast UniFrac metric and OrthoANI values revealed that bacterial communities in ATL1 and ATL2 were closely related, but both communities were distantly related to the ATL3 (Fig. A4). Nevertheless, evolutionary relatedness of the bacterial taxa defined by OTUs via CD-HIT and sample radius by Shannon was depicted by PCoA coordinates, which corroborated some relatedness between ATL1 and ATL2 based on numbers of OTUs shared among the two locations, and their dissimilarity from ATL3 since they did not ordinate alike (Fig. 4).

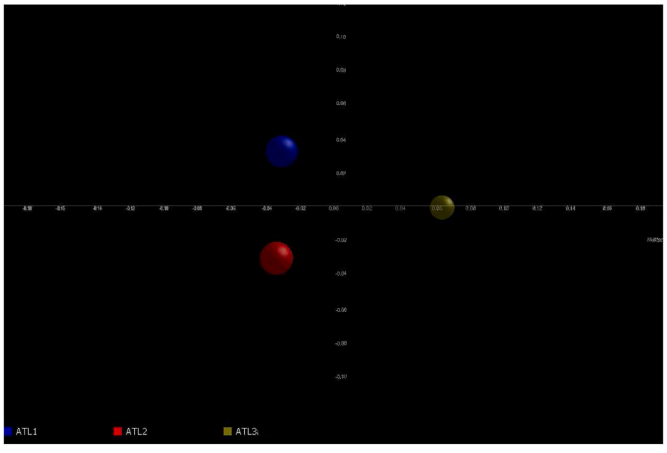

Fig. 4. The relatedness of bacterial communities between the oceanic (ATL1 and ATL2) and estuarine (ATL3) sediments, using principal coordinate analysis (PCoA) based on weighted UniFrac parameters that are normalized and treated unclassified operational taxonomic units (OTUs). OTUs are defined by CD-HIT and radius is Shannon.

Canonical correspondence analysis (CCA) did not only further establish that the sampling locations ordinate differently but more importantly revealed that PHs shaped bacterial assemblage of ATL1 while HMs determined the bacterial community of ATL3 (Fig. 5). Both PHs and HMs variables appeared not to have influences on bacterial community of ATL2. The X-axis of the CCA bi-plot resolved the geographic differences of ATL1 and ATL2 by 91.2% variance. The bacterial communities in relation to environmental fluxes were subdivided across a slope gradient through 8.7% variability. It is of note that phenanthrene and anthracene exerted equal influence on bacteria assemblage in ATL1 as they visibly ordinate along the same vector. However, the duo (phenanthrene and anthracene) highly correlate with pyrene but partially correlate with naphthalene to shape the bacterial community in ATL1. Nevertheless, Cd highly correlated with Pb, and both HMs distantly correlated with Zn to characterise the bacteria assemblage of ATL3. It can be inferred that the PHs and HMs were poorly correlated in driving the bacteria profile of ATL1 and ATL3 as shown through the wide degree the factors ordinated.

4. Discussion

Pollution of marine environment with petroleum hydrocarbon (PH) remains a global phenomenon that constitutes hazards to marine health. Anthropogenic sources of PHs at the Atlas Cove on the Atlantic Ocean include leaking pipelines, discharges from loading and off-loading, and run-off from loading platform. The physico-chemistry at the sites exceeding the recommended permissible limits of environmental guidelines is an evident of anthropogenic activities, which have variously been reported (Oyetibo et al, 2010, 2019; Sogbanmu et al., 2019). The low risk index of total petroleum hydrocarbon (TPH) at the sites can be explained to be due to natural attenuation phenomena in the environments. It is noteworthy that ecological risk index of TPH was higher in ATL1, which consistently receives certain volumes of petroleum cuts unlike in few kilometres away from the petroleum loading facility (ATL2) where the PH contaminations might have been dispersed. However, TPH risk index in ATL3 remained highest probably due to indiscriminate discharge of petroleum products from multiple sources since environmental regulations were apparently at low ebb. Moreover, high eco-risk indexes of determined PAHs, except fluorene, at all the sites depict possible mass transfer of the PAHs from the sediments to aquatic life, leading to bioaccumulation in the tissues of the aquatic life and eventual biomagnifications along the trophic levels. Similar phenomena have been previously reported in estuarine ecosystems (Sogbanmu et al., 2019). The partitioning of the toxicants (PHs, HMs and PAHs) between the sediments and the water phase of an oceanic water-sediment system at equilibrium indicates the strength of sorption of the toxicants to sediment and eventually into the bacterial community (Oyetibo et al., 2016). The partitioning coefficient values of the toxicant are inversely proportional to the ecological risk index quotients. This revealed that fluorene is more strongly sorb onto the sediment from water phase unlike other PAHs, imparting the bacterial community. Thus, partitioning coefficients of the toxicants vary with the organic contents of the sediment as determined by index risk quotient, providing basis for comparing distribution of the toxicants. As such, phenanthrene, anthracene and pyrene posed the strongest ecological risk to aquatic life in sediments of the petroleum loading facility (ATL1) and some distance away (ATL2) due to continual release of the compounds into the ecosystem. On the contrary, phenanthrene, anthracene and pyrene were of less risk to life in the estuarine (ATL3) sediment since their influx might likely not surpass their degradation rate. Similarly, high eco-risk of Zn, Cu, Ni and Cr may be due to their linkage with PH and thus co-exist at the sites upon PH discharge.

Bacterial assemblages in marine milieu respond rapidly to PH toxicity in terms of diversity, physiology and functional characteristics (Aylagas et al., 2017; Lozada et al., 2014) with extinction of sensitive genres and superflux of hydrocarbonoclastic taxa. Knowing that bacterial community structure of the polluted marine system determines and

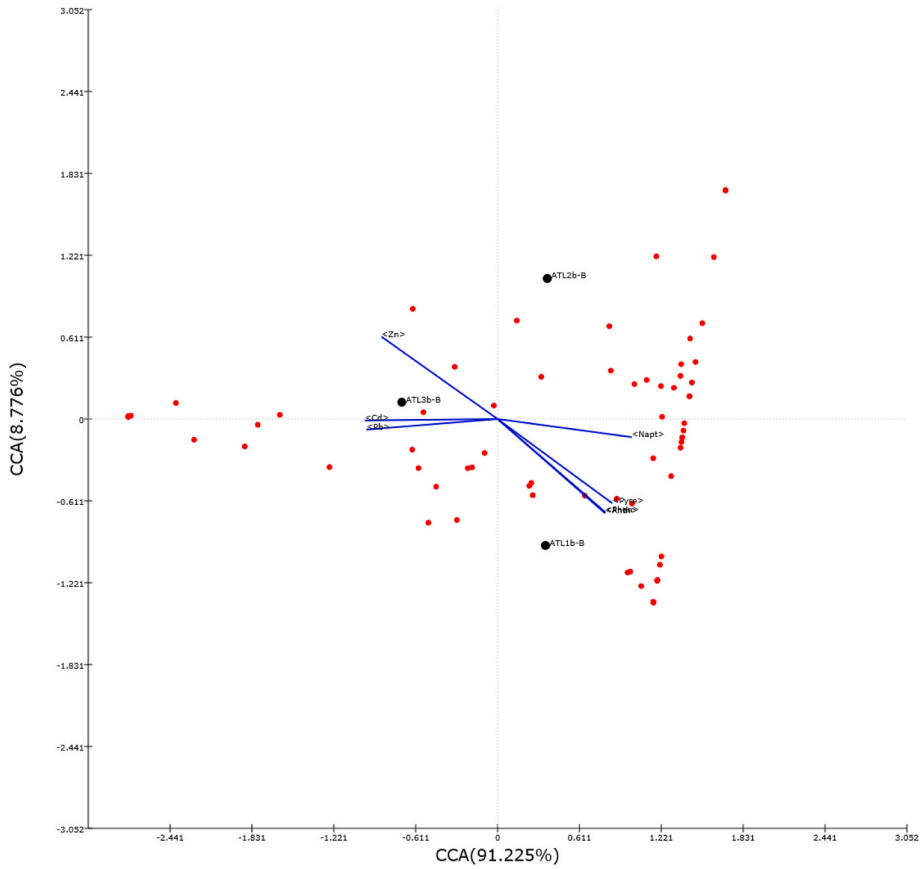

Fig. 5. Canonical correspondence analysis two-axis plot of marine stressors on the bacterial community. The vectors represent statistically significant cluster-dominating variables explaining the observed patterns ($p < 0.05$). The two axes represent 91.2%–8.8% of variability.

drives the functions of the ecosystem, a drift in the bacterial profile that cascaded to the emergence of dominant phyla with characteristic ability to degrade PHs is required in the self-recovery processes of the contaminated system. The presence of Latescibacteria_WS3 and other members of the Fibrobacteres-Chlorobi-Bacteroidetes superfamily, among the 11 phyla (whose sum sequence read were greater than 5%) have been reportedly contributing to anoxic carbon cycling via hydrocarbon degradation along with other complex carbon vagaries in marine sediments (Dombrowski et al., 2017; Youssef et al., 2015). Despite the ubiquitous distribution of Latescibacteria_WS3, the low abundance of members of this phylum in ATL1 (1.7 ± 0.4%), ATL2 (1.4 ± 0.04%) and ATL3 (0.13 ± 0.03%) corroborate previous reports (Farag et al., 2017). Bacteroidetes that was equally found among the dominant phyla in this study have been reportedly present in hydrocarbon-contaminated environments but without direct linkage to hydrocarbon degradation (Acosta-Gonzalez and Marques, 2016). Members of Chloroflexi, Plantomycetes and Acidobacteria phyla are abundant and represent a significant proportion of the bacterial community in the sea ecosystem as found in this study, although, their ecological role still remain vague (Fuerst, 2017). Interestingly, Plantomycetes and Acidobacteria that constituted more than 5% sequence reads in the oceanic sediments but less than 1% in the estuarine sediment prefer copiotrophic conditions (Oyetibo et al., 2019), and might not be relevant in degradation of PHs.

The dominance of Proteobacteria in the sediments as projected through γ-, δ-, and α-Proteobacteria, indicate plausible role they play regarding metabolism of PHs. The abilities of α- and γ-Proteobacteria to mineralise PHs have been previously established, where γ-Proteobacteria, as observed in the present study, was found to be the most abundant bacterial groups in marine sediments (Acosta-Gonzalez et al., 2013). Members of γ-Proteobacteria are reportedly by far most abundant and known to contribute to the early stages of PHs degradation, while those of δ-Proteobacteria often play a key role in the anaerobic degradation of PHs. It is noteworthy that low abundances of ε-Proteobacteria and β-Proteobacteria in the oceanic sediments in relation to relatively high sequence reads (19.2% and 9.0%, respectively) in the estuarine sediment suggests the pivotal role the members of these taxa might be playing in the physiology of the ecosystem. Kostka et al. (2011) had reported similar pronounced shift in bacterial taxa in response to PHs contamination. At genus level, *Sulfurimonas* and *Woeseia* predominating oceanic ATL2 and estuarine ATL3 sediments, respectively, might be involved in sulphur biogeochemistry along with PHs degradation in the ecosystems. The ecological roles with respect to PHs metabolism of a number of unidentified, not yet cultured genera found among the most dominant genera cannot be ascertain yet, but their dominance must be pivotal to self-recovery processes taking place in the sediments. Abundance of *Parvibaculum* in ATL1 indicates availability of PHs, particularly the PAHs in the environment as previously been reported (Lai et al., 2011). Nevertheless, taxa within *Parvibaculum* have been reportedly playing crucial roles in PH-degradation process in contaminated sediments (Looper et al., 2013). Applicability of the dominant bacterial OTUs is anticipated sustainable enhanced bioremediation of the polluted marine waters is achievable via integration of circular economy concept within the bacteria-induced self-recovery processes (Kapsalis et al., 2019). Several novel approaches including coupling the dominant bacterial OTUs to composite materials (Zamparas et al., 2019, 2020) follow by packaging in water-permeable bags in form of "teabags' (Zamparas et al., 2020) could be adopted to managing identified eco-toxicants in the polluted marine environment.

Based on the pollution level of the samples, differences in diversity among the sediments depict varied degree of pollution where a decrease in diversity is associated with higher levels of pollution. Alpha diversity metrics (Chao1, Ace and Shannon indices) confirmed that the oceanic

sediments are less polluted than that of the estuarine, containing more diverse bacteria taxa. Lesser diverse OTUs in estuarine sediment must be due to multifarious human activities plus PHs pollution, without constant physical mixings and dilutions physiognomies of the oceanic environments. Furthermore, dissimilarity of the oceanic sediments (ATL1 and ATL2) and estuarine sediment (ATL3) indicates the heterogeneity of these ecosystems. UPGMA dendogram and the principal coordinate analysis (PCoA) coordinates depicted close relationship of ATL1 and ATL2, sharing a large numbers of OTUs that are distantly related to the OTUs found in ATL3. Higher number of OTUs (species richness) suggests richer genetic diversity in the oceanic sediments than what was observed in the estuarine sediment. Even at that, the Atlas Cove sediment (ATL1) was observed less diverse and not as rich as ATL2 since ATL1 is exposed to PHs contamination that would have sunk into the sediment impacting sensitive populations. Bacteria diversity found in ATL1 and ATL2 is inversely proportional to the degree of petroleum hydrocarbon influence as equally reported previously (Rosano--Hernandez et al., 2012; Catania et al., 2018). Correlations between physio-chemical parameters and operational parameters, along with diversity, performance and functionalities of bacteria in ecosystems as determined by CCA have variously been discussed (Jiang et al., 2018). Although there is paucity of data correlating geochemical factors and metagenomes pivotal to eco-metabolism of PHs through dominant taxa in polluted marine ecosystem, the results obtained in the current study showcased component of a conceptual circular economy model for the management of marine pollution worldwide (Zamparas et al., 2020). However, CCA was able to resolve dissimilarity between ATL1 and ATL2 that seemingly similar via UPGMA dendogram since the two locations were split by 91.2% variability despite their geographic proximity. Furthermore, the joint plot of CCA in this study revealed that phenanthrene, anthracene and pyrene drove the bacteria profile in ATL1, while Pb, Cd and Zn shaped the bacteria community in ATL3, on contrary to ATL2 that was apparently unaffected by the geochemical fluxes. Altogether, the dominant OTUs spurred by coexistence of the geochemical factors, HMs and PHs are poised as prospective biotechnological tools in sustainable decommissioning strategies applicable to contaminated marine waters, thereby taunting marine conservation/protection globally.

5. Conclusion

Forty four bacterial phyla, dominated with Proteobacteria, Chloroflexi, Plantomycetes, Acidobacteria and Bacteriodetes were profiled in the oceanic sediments exposed to petroleum contamination during transportation. The oceanic sediments contained richer and more diverse bacterial community than sediments of estuarine exposed to multiple sources of contamination. The OTUs of the bacteria revealed close relationship in the oceanic sediments from different sampling locations, but distantly related to the OTUs found in estuarine sediments. PHs determined bacteria assemblage in ATL1 where petroleum transport occurred unlike in ATL2 that is distanced away from petroleum transportation, while HMs shaped the bacteria community at the estuarine systems. The dominant bacteria taxa including unclassified *DQ811856_g, Woeseia* and *Sulfurimonas* are therefore suggested to be the key players in the natural attenuation of the contaminated marine ecosystem. Thus, the dominant taxa would be a good biotechnological tool applicable to drive bio-augmentation strategies of the ocean where petroleum transportation occurs. Nevertheless, the extinct 210 bacterial genera were suggested to be bio-indicators of respective petroleum hydrocarbons and heavy metals pollution that drive the autochthonous bacterial community.

Authors' contribution

GOO participated in experimental design, supervising experimentation, interpretation of data, and manuscript preparation; OOI participated in sample collection, experimentation, data collation and manuscript preparation; PKO participated in experimentation and data collation; OOA participated in interpretation of data and manuscript preparation.

Declaration of competing interest

The authors declare that they have no known competing financial interests or personal relationships that could have appeared to influence the work reported in this paper.

Appendix A. Supplementary data

Supplementary data to this article can be found online at https://doi.org/10.1016/j.jenvman.2021.112563.

References

Acosta-Gonzalez, A., Marques, S., 2016. Bacterial diversity in oil-polluted marine coastal sediments. Curr. Opin. Biotechnol. 38, 24–32.

Acosta-Gonzalez, A., Rossello-Mora, R., Marques, S., 2013. Characterization of the anaerobic microbial community in oil-polluted subtidal sediments: aromatic biodegradation potential after the Prestige oil spill. Environ. Microbiol. 15, 77–92.

Aylagas, E., Borja, A., Tangherlini, M., Dell'Anno, A., Corinaldesi, C., Michell, C.T., Irigolen, X., Danovaro, R., Rodriguez-Ezpeleta, N., 2017. A bacterial community-based index to assess the ecological status of estuarine and coastal environments. Mar. Pollut. Bull. 114, 679–688.

Barin, R., Talebi, M., Biria, D., Beheshti, M., 2014. Fast bioremediation of petroleum contaminated soils by a consortium of biosurfactant/bioemulsifier producing bacteria. Int. J. Environ. Sci. Technol. 11, 1701–1710.

Brooijmans, R.J.W., Pastink, M.J., Siezen, R.J., 2009. Hydrocarbon-degrading bacteria: the oil-spill clean-up crew. Microb. Biotechnol. 2, 587–594.

Catania, V., Cappello, S., Di Giorgi, V., Santina, S., Di Maria, R., Mazzola, A., Vizzini, S., Quatrini, P., 2018. Microbial communities of polluted sub-surface marine sediments. Mar. Pollut. Bull. 131, 396–406.

Catania, V., Santisi, S., Signa, G., Vizzini, S., Mazzola, A., Cappello, S., Yakimov, M.M., Quatrini, P., 2015. Intrinsic bioremediation potential of a chronically polluted marine coastal area. Mar. Pollut. Bull. 99, 138–149.

Desforges, J.W., Sonne, C., Levin, M., Siebert, U., Guise, S.D., Dietz, R., 2016. Immunotoxic effects of environmental pollutants in marine mammals. Environ. Int. 86, 126–139.

Dombrowski, N., Seitz, K.W., Teske, A.P., Baker, B.J., 2017. Genomic insights into potential interdependencies in microbial hydrocarbon and nutrient cycling in hydrothermal sediments. Microbiome 5, 106. https://doi.org/10.1186/s40168-017-0322-2.

Duran, R., Gravo-Laureau, C., 2016. Role of environmental factors and microorganisms in determining the fate of polycyclic aromatic hydrocarbons in the marine environment. FEMS Microbiol. Rev. 40, 814–830.

Farag, I.F., Youssef, N.H., Elshahed, M.S., 2017. Global distribution patterns and pangenomic diversity of the Candidate phylum "Latescibacteria" (WS3). Appl. Environ. Microbiol. 83 (10) https://doi.org/10.1128/AEM.00521-17.

Fuerst, J.A., 2017. Planctomycetes – new models for microbial cells and activities. Microbial Resour. https://doi.org/10.1016/B978-0-12-804765-1.00001-1.

Head, L.M., Jones, O.M., Roling, W.F., 2006. Marine microorganisms make a meal of oil. Nat. Rev. Microbiol. 4, 173–182.

Jiang, X.-T., Ye, L., Ju, F., Li, B., Ma, L.-P., Zhang, T., 2018. Temporal dynamics of activated sludge bacterial communities in two diversity variant full-scale sewage treatment plants. Appl. Microbiol. Biotechnol. https://doi.org/10.1007/s00253-018-9287-8.

Kapsalis, V.C., Kyriakopoulos, G.I., Aravossis, K.G., 2019. Investigation of ecosystem services and circular economy interactions under an inter-organizational framework. Energies 12, 1934. https://doi.org/10.3390/en12091734.

Kostka, J.E., Prakash, O., Overholt, W.A., Green, S.J., Freyer, G., Canion, A., Delgardio, J., Norton, N., Hazen, T.C., Huettel, M., 2011. Hydrocarbon-degrading bacteria and the bacterial community response in Gulf of Mexico beach sands impacted by the Deep-water Horizon oil spill. Appl. Environ. Microbiol. 77, 7962–7974.

Lai, Q., Wang, L., Liu, Y., Yuan, J., Sun, F., Shao, Z., 2011. *Parvibaculum indicum* sp. nov., isolated from deep-sea water. Int. J. Syst. Evol. Microbiol. 61, 271–274.

Looper, J.K., Cotto, A., Kim, B.Y., Lee, M.K., Liles, M.R., Ni Chadhain, S.M., Son, A., 2013. Microbial community analysis of Deepwater Horizon oil-spill impacted sites along the Gulf coast using functional and phylogenetic markers. Environ. Sci. Process Impacts 15, 2068–2079.

Lozada, M., Marcos, M.S., Commendatore, M.G., Gil, M.N., Dionisi, H.M., 2014. The bacterial community structure of hydrocarbon-polluted marine environments as the basis for the definition of an ecological index of hydrocarbon exposure. Microb. Environ. 29 (3), 269–276.

Nguyen, N.-L., Kim, Y.-J., Hoang, V.-A., Subramaniyam, S., Kang, J.-P., Kang, C.H., Yang, D.-C., 2016. Bacterial diversity and community structure in Korean Ginseng field soil are shifted by cultivation time. PloS One 11 (5), e0155055. https://doi.org/10.1371/journal.pone.0155055.

Obayori, O.S., Ilori, M.O., Adebusoye, S.A., Oyetibo, G.O., Omotayo, A.E., Amund, O.O., 2009. Degradation of hydrocarbons and biosurfactant production *Pseudomonas* sp. strain LP1. World J. Microbiol. Biotechnol. 25, 1615–1623.

Ogwugwa, V.H., Oyetibo, G.O., Amund, O.O., 2020. Taxonomic profiling of bacteria and fungi in freshwater sewer receiving hospital wastewater. Environ. Res., 110319 https://doi.org/10.1016/j.envres.2020.110319.

Oyetibo, G.O., Chien, M.-F., Otsubo, W., Obayori, O.S., Adebusoye, S.A., Ilori, M.O., Endo, G., 2017. Biodegradation of crude oil and phenanthrene by heavy metal resistant Bacillus subtilis isolated from multi-polluted environments. Int. Biodeterior. Biodegrad. 120, 143–151.

Oyetibo, G.O., Ilori, M.O., Adebusoye, S.A., Obayori, O.S., Amund, O.O., 2010. Bacteria with dual resistance to elevated concentrations of heavy metals and antibiotics in Nigerian contaminated systems. Environ. Monit. Assess. 168, 305–314.

Oyetibo, G.O., Ilori, M.O., Obayori, O.S., Amund, O.O., 2013. Biodegradation of petroleum hydrocarbons in the presence of nickel and cobalt. J. Basic Microbiol. 53, 1–11. https://doi.org/10.1002/jobm.201200151.

Oyetibo, G.O., Miyauchi, K., Huang, Y., Ikeda-Ohtsubo, W., Chien, M.-F., Ilori, M.O., Amund, O.O., Endo, G., 2019. Comparative geochemical evaluation of toxic metals pollution and bacterial communities of industrial effluent tributary and a receiving estuary in Nigeria. Chemosphere 227, 638–646.

Oyetibo, G.O., Miyauchi, K., Suzuki, H., Endo, G., 2016. Extracellular mercury sequestration by exopolymeric substances produced by *Yarrowia* spp. during growth: thermodynamics, mass action equilibrium, and kinetics studies. J. Biosci. Bioeng. 122, 701–707.

Rosano-Hernandez, M.C., Ramirez-Saad, H., Fernandez-Linares, L., 2012. J. Environ. Manag. 95, S325–S331.

She, S., Niu, J., Zhang, C., Xiao, Y., Chen, W., Dai, L., Liu, X., Yin, H., 2017. Significant relationship between soil bacterial community structure and incidence of bacterial wilt disease under continuous cropping system. Arch. Microbiol. 199, 267–275. https://doi.org/10.1007/s00203-016-1301-x.

Sogbanmu, T.O., Osibona, A.O., Otitoloju, A.A., 2019. Specific polycyclic aromatic hydrocarbons identified as ecological risk factors in the Lagos lagoon, Nigeria. Environ. Pollut. 255, 113295–113304.

Varjani, S.J., 2017. Microbial degradation of petroleum hydrocarbons. Bioresour. Technol. 223, 277–286.

Ventikos, N.P., Sotiropoulos, F.S., 2014. Disutility analysis of oil spills: graphs and trends. Mar. Pollut. Bull. 81, 116–123.

Yoon, S.H., Ha, S.M., Kwon, S., Lim, J., Kim, Y., Seo, H., et al., 2017. Introducing EzBioCloud: a taxonomically united database of 16S rRNA and whole genome assemblies. Int. J. Syst. Evol. Microbiol. 67, 1613–1617.

Youssef, N.H., Farag, I.F., Rinke, C., Hallan, S.J., Woyke, T., Elshahed, M.S., 2015. *In silico* analysis of the metabolic potential and niche specialization of Candidate phylum "Latescibacteria" (WS3). PloS One 10 (6), e0127499. https://doi.org/10.1371/journal.pone.0127499.

Zamparas, M., Kyriakopoulos, G.L., Drosos, M., Kapsalis, V.C., Kalavrouziotis, I.K., 2020. Novel composite material for lake restoration: a new approach impacting on ecology and circular economy. Sustainability 12, 3397. https://doi.org/10.3390/su12083397.

Zamparas, M., Kyriakopoulos, G.L., Kapsalis, V.C., Drosos, M., Kalavrouziotis, I.K., 2019. Application of novel composite materials as sediment capping agents: column experiments and modelling. Desalin. Water Treat. 170, 111–118. https://doi.org/10.5004/dwt.2019.24909.